Low-Power Radio-Frequency Ion Thruster

IEPC-2015-322／ISTS-2015-b-322

*Presented at Joint Conference of 30th International Symposium on Space Technology and Science
34th International Electric Propulsion Conference and 6th Nano-satellite Symposium,
Hyogo-Kobe, Japan
July 4 – 10, 2015*

Nikolay N. Antropov[1], Ruslan V. Akhmetzhanov[2], Aleksandr V. Bogatyi[3], Grigoriy A. Dyakonov[4], Garri A. Popov[5]
Research Institute of Applied Mechanics and Electrodynamics of Moscow Aviation Institute (National Research University), 125080 Moscow, Russia

Albert I. Belogurov[6], Pavel A. Dronov[7], Andrey V. Ivanov[8]
OSC "Konstruktorskoe Buro Khimavtomatiky", 394006 Voronezh, Russia

Sergey A. Khartov[9]
Moscow Aviation Institute (National Research University), 125993 Moscow, Russia

The report is devoted to the development and experimental refining of low-power radio-frequency ion thruster at the Moscow Aviation Institute. To substantiate characteristics, the computational studies were performed, which allowed determining the design parameters of the screen and accelerating electrodes and other elements of the thruster. Thermal calculation of the low-power radio-frequency ion thruster (RIT) was made to identify the most heat-stressed thruster components. Calculation of the thermomechanical stability of the ion-extraction system electrodes of molybdenum and titanium was made. The design of the thruster unit was developed. An experimental model of the thruster was developed and tested.

Nomenclature

N	=	total power consumption of the thruster
P	=	thrust
I_{sp}	=	specific impulse
g_0	=	gravitational acceleration
η	=	thruster efficiency
η_α	=	divergence efficiency
i	=	ion beam current
M	=	the atomic mass of the working fluid
q	=	ion charge
U_+	=	potential of the screen grid
U_p	=	plasma potential
η_m	=	mass efficiency
j_i	=	ion beam current density

[1] Leading researcher, Department 13, riame3@sokol.ru
[2] Engineer, Department 13, ahmetzhanov1991@mail.ru
[3] Researcher, Department 13, boga-alex@ya.ru
[4] Senior researcher, Department 13, riame3@sokol.ru
[5] Chief designer, Director, riame@sokol.ru
[6] Deputy chief designer, cadb@comch.ru
[7] Head of group, cadb@comch.ru
[8] Chief designer, cadb@comch.ru
[9] Professor, Department of Electric Propulsions and Power Plants, skhartov@yandex.ru

e = elementary charge
n_e = electron density
T_e = electron temperature
ε_j = emissivity factor of surface elements
δ_{ij} = Kronecker delta
A_i = elementary area
σ = Stefan-Boltzmann constant
q_{ji}^{Rad} = radiant flux density
n_i = plasma density
q_{ji}^{Cond} = heat conductive flux density
w_j^{Plasma} = power flux density

I. Introduction

In recent years the number of small satellites injected into orbit increased vastly. The cost of small satellites is significantly lower than the cost of heavy satellites that reduces losses in case of a failed launch or early failure during operation[1]. Because of the relative simplicity of small satellites, duration of time period for their designing and manufacturing are shorter significantly. The analysis of modern trends of spacecraft market shows[2] that the operation of a number of systems can be provided by small satellites from 100 kg to 500 kg in mass placed in the low, up to 1000 km, orbits. They include systems of mobile communication and radio navigation and systems of Earth, atmosphere and near space monitoring. The share of launched heavy spacecraft (weighing 1 ton and above) is decreasing continuously and comprises now no more than 30% of the total number of launched spacecraft[3].

Opinion about the fields, in which small satellites can be used, has recently changed substantially. Thus, small satellites are finding increasing use for solving communication and broadcasting problems, in GEO including. Currently, not less than 25% of geostationary satellites have a mass less than 500 kg [2,4].

For the return of investments into the problems solved by small satellites weighing 150 ... 600 kg, we need to extend their lifetime up to 5 ... 10 years[5]. It is necessary to equip small satellites with low-power (up to 500 W) electric propulsions for that. RIT with the power of 150 ... 500 W can be used as such.

II. Calculation of the thruster main performance data and design parameters

A. The scheme of thruster operation

RIT operates as follows. The plasma-forming gas xenon is fed into the discharge chamber. Radiofrequency (RF) power is applied from the RF generator to the inductor. The discharge ignition is initiated by a short-term feed of electrons emitted by the neutralizer into the discharge chamber. After the ignition, the RF discharge of inductive type is maintained in the discharge chamber. Electrons heated by RF electromagnetic field ionize working fluid in the discharge. Ions are extracted from the discharge plasma and accelerated in the ion-extraction system. In the stationary operating mode the neutralizer is used for the injection of electrons into the beam of accelerated ions; this provides current neutralization of the plasma jet[6]. RIT operation is illustrated by Figure 1.

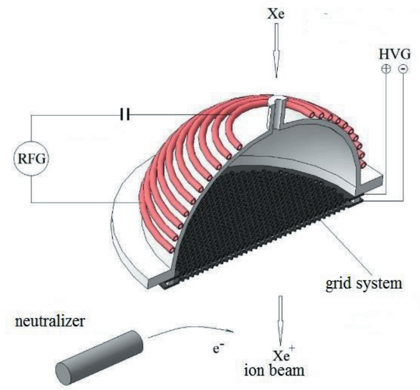

Figure 1. Scheme of RIT work

Structural scheme of a three-electrode ion-extraction system, in which the scheme of ions "acceleration-deceleration" is implemented, is shown in Figure 2. Two electrodes – screen and accelerating – are perforated with a lot of coaxial holes. The third decelerating electrode is usually made as a ring encircling the beam, or it may be perforated also. Potential of the screen electrode is positive; potential of the accelerating electrode is negative relative to the body. Decelerating electrode is grounded or is under the potential of the satellite body[7].

The ions are extracted from the quasi-neutral plasma of gas discharge in the discharge chamber through the holes in the screen electrode and are accelerated by a potential difference between screen electrode and accelerating electrode. Formation of ion beam with certain energy, current density and geometry is achieved by matching the discharge plasma parameters (plasma density and electron temperature) with the geometric parameters of the grid system (hole diameters, electrode thickness, and interelectrode gap), as well as with electric potentials of screen electrode and accelerating electrode and the atomic mass of the propellant.

Ion beam is transformed into a quasineutral plasma flow in the neutralization zone. Plasma potential in the neutralization zone reaches the steady state automatically in such a way that a potential trap is formed for retaining electrons compensating space charge of ions in its volume[7].

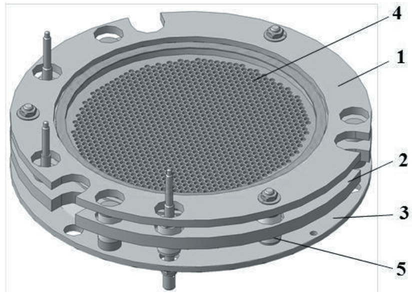

Figure 2. Constructive scheme of the grid system

1 – support flange of the screen grid; 2 – support flange of the accelerating grid; 3 – support flange of the decelerating grid; 4 – screen grid; 5 – clamping unit

B. Calculation of the main characteristics of RIT

Main characteristics of RIT are the thrust P (in N), specific impulse I_{sp} (in s), and efficiency η. These values are linked by Eq. (1):

$$N = \frac{P \cdot I_{sp} \cdot g_0}{2\eta} \quad (1)$$

where N is the total power consumption of the thruster, g_0 is the gravitational acceleration.

Thrust is calculated by Eq. (2):

$$P = \eta_\alpha \cdot i \cdot \sqrt{2 \cdot \frac{M}{q} \cdot \left(U_+ + U_p\right)} \quad (2)$$

where η_α – divergence efficiency, defining the loss in the creation of directional thrust due to the beam divergence, i – ion beam current, q – ion charge, M – the atomic mass of propellant (in this case we use xenon), U_+ – potential of the screen electrode relative to the thruster casing, U_p – potential of plasma in the discharge chamber relative to the screen electrode.

Specific impulse is calculated as follows (Eq. 3):

$$I_{sp} = \frac{\eta_m}{g_0} \cdot \sqrt{2 \cdot \frac{q}{M} \cdot \left(U_+ + U_p\right)} \quad (3)$$

where η_m is the propellant mass efficiency, which is equal to the coefficient of xenon ionization in the discharge chamber.

Basic characteristics of the low-power RIT were calculated by these formulas for the power consumption of 300 W taking into consideration the ionization cost and ionization coefficient[8]. These characteristics are presented in Table 1.

Accelerating voltage , V	Thrust, mN	Specific impulse, s	Efficiency	Ion beam current, mA	Propellant mass flow, mg/s	RF power, W
1000	10.6	2770	0.48	208	0.398	82
1500	9.6	3300	0.52	153	0.300	60
2000	8.8	3715	0.53	121	0.244	48
2500	8.1	4050	0.54	100	0.207	39

Table 1. Calculated characteristics of low-power RIT

Operating mode with accelerating voltage of 2000 V was selected as the basic.

C. Calculation of basic geometrical parameters of the grid system

Let us consider an elementary hole of the grid system. There may be from several tens to several thousands of such holes in the grid system depending on the size and required characteristics of the thruster. Two neighboring holes are shown in Figure 3. The current density of the ion beam through the elementary hole is estimated using Eq. (4)[9].

$$j_i \approx 0{,}43 e n_e \sqrt{\frac{2T_e}{M}} \quad (4)$$

where j_i – ion current density, e – elementary charge, n_e – electron density, T_e – electron temperature in the discharge chamber, M – the atomic mass of ion. Plasma potential U_p relative to the screen grid is estimated[10] using Eq. (5).

$$U_p \approx -\frac{T_e}{e}\ln\left(0.86\cdot\sqrt{\frac{\pi\cdot m_e}{M}}\right) \quad (5)$$

where m_e is the electron mass.

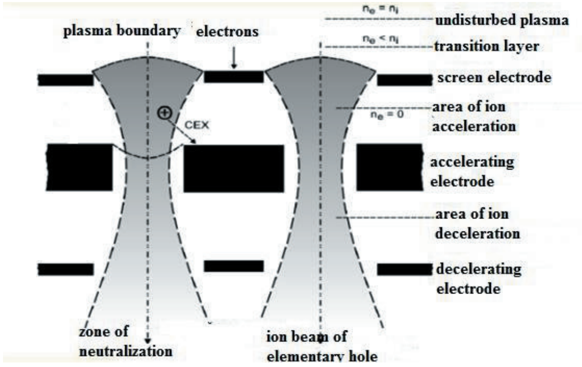

Figure 3. Elementary holes of the grid system

Mathematical model of the primary beam is described by Eq. (6-8) [10]:

1) Poisson equation describing electric field generated by electrodes with the given potentials and space charge of the primary beam:

$$\Delta\varphi = \left(\frac{\partial^2\varphi}{\partial r^2} + \frac{1}{r}\frac{\partial\varphi}{\partial r} + \frac{\partial^2\varphi}{\partial z^2}\right) = \frac{j_i}{\varepsilon_0\sqrt{2e\varphi/M}} \quad (6)$$

2) The equation of motion of positively charged particles in the electrostatic field:

$$M\frac{d\upsilon}{dt} = -e\cdot grad(\varphi) \quad (7)$$

3) Continuity condition, according to which primary beam ions in the interelectrode gap can neither originate nor disappear:

$$div(e\cdot n_i\cdot\varphi) = 0 \quad (8)$$

where n_i – plasma density.

The following boundary conditions are imposed on this system of equations:

– electrode potential in each its point is identical, the geometry of the electrodes remains unchanged;

– on the axis of symmetry in the direction of normal to the axis grad(φ)=0 (Neumann condition);

– the potential distribution in the transition layer [11];

– the boundary of the primary ion beam neutralization zone.

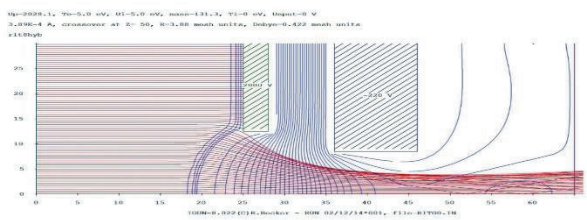

Figure 4. Calculation of elementary hole of the grid system in software package IGUN

This problem is solved using the software package IGUN[12]. While modeling ion flow in IGUN, the following inputs are used: geometric parameters of the grid system, potentials of the electrodes, the atomic mass of the propellant (in our case, it is 131.3 amu for xenon), electron temperature in the discharge chamber. Besides, it is necessary to introduce either the ion current density through the elementary hole, or the plasma density in the discharge chamber. The geometrical parameters of the grid system are selected based on the following considerations:

– thickness of the screen electrode is selected to be as low as practicable for the reduction of the propellant ionization cost[8];

– interelectrode gap should be selected in such a way as to prevent the grid system breakdown. Its size depends on the potential difference between the electrodes and the materials of which the electrodes are made[13].

The electron temperature is taken to be 5 eV[8]. The potential of the screen grid is taken to be 2000 V. The potential of the accelerating electrode is negative and its absolute value should be 10-11% of the potential of the screen electrode[8]. While modeling in IGUN, the following data are the outputs: beam current through the elementary hole, distribution of space charge, ion trajectories and half-angle of the ion beam divergence.

Calculations for various configurations of the grid system were made, and finally we selected the grid system with the most narrow half-angle of divergence (11 degrees) and the following geometrical parameters: thickness of the screen electrode - 0.3 mm, thickness of the accelerating electrode - 1.5 mm, interelectrode gap - 0.8 mm, diameter of holes in the screen electrode - 2.5 mm, diameter of holes in the accelerating electrode - 1.7 mm. The ring-shaped decelerating electrode was selected in that case. With such input data, the ion beam current through the elementary hole was 0.389 mA. With the total ion beam current of 121 mA, there should be 313 elementary holes in the grid system. IGUN calculation result for the elementary hole of the grid system is shown in Figure 4.

D. Thermal modeling

In the thermal modeling it was accepted that the heat exchange between the construction elements was either by emission or by thermal conductivity. For all coupling surfaces, thermal contact resistances in accordance with the thermal conductivity and roughness of the contacting surfaces and the contact pressure were preliminary calculated[14].

The method of discrete elements was used for solving the problem. The object of research was divided into a large number of small elements, within which all the physical characteristics, especially the temperature, are identical. The accuracy of the method is defined by the number of elements N that is limited by the throughput of applied computational tools. The number of mesh elements was about 70000.

In the calculation model, a system of linear algebraic equations (Eq.(9)) for the flows of radiant energy Q_i coming from each i-th surface element is solved[15]:

$$\sum_{i=1}^{N}\left(\frac{\delta_{ji}}{\varepsilon_i} - F_{ji}\frac{1-\varepsilon_i}{\varepsilon_i}\right)\frac{1}{A_i}Q_i = \sum_{i=1}^{N}\left(\delta_{ji} - F_{ji}\right)\sigma T_i^4 \qquad (9)$$

where ε_j – emissivity factor of surface elements; δ_{ij} – Kronecker delta; A_i – square areas of the relevant elements; σ – Stefan-Boltzmann constant.

Heat balance equation for the i-th mesh element in view of the heat power coming from the discharge chamber plasma, radiant and heat-conductive heat exchange between various elements of the RIT partition mesh can be represented by Eq. (10):

$$q_i = \sum(q_{ji}^{Rad} + q_{ji}^{Cond}) + w_j^{Plasma} \qquad (10)$$

where q_i – density of the thermal power flux emanating from the i-th element of the partition mesh, q_{ji}^{Rad} – density of the total radiant flux coming to the i-th element, summed over all elements j, q_{ji}^{Cond} – density of the heat-conducting flow coming to the i-th element from j-elements adjacent to the i-th one, w_j^{Plasma} – density of the corresponding power flux coming from the plasma onto the i-th element.

The heat-conducting flow q_{ji}^{Cond} between the elements i and j is defined by a finite-difference expression of conventional Fourier law of heat conduction, wherein the temperature difference between adjacent elements related to the effective distance between the elements, is used in place of the temperature gradient.

Thermal calculation for two variants of the grid system was performed: for the electrodes made of titanium and of molybdenum. The titanium screen grid was heated up to 345°C in the center and was the most heated of the thruster components. It should be noted that the temperature difference from the center to the edge of the titanium electrode was about 100 °C; this may result in the electrode deformation during the thruster operation. The molybdenum screen electrode was heated up to 265°C in the center, and the temperature difference was 30°C. Accelerating electrodes made of titanium and molybdenum were heated up to 165°C and 150°C respectively, with the temperature differences of a few degrees.

Concerning other constructional elements, the most heated was the discharge chamber, which was heated up to 240°C. The inductor was heated by thermal flux from the discharge chamber; its temperature was 220°C.

Among the construction elements, from the external surfaces of which the main heat release from the thruster into the surrounding space by emission takes place, the most heated (up to 220 °C) was the part of the load-carrying ring, to which the discharge chamber and the screen electrode were mounted. Despite the small thickness and low heat conductivity of ceramic walls of the discharge chamber, the load-carrying ring in this part accumulates significant amount of heat "flowing down" to it from the walls of the discharge chamber and the screen electrode. Temperatures of mounting surfaces by which the ionic part of RIT is mechanically interfaced with other elements of the propulsion system are about 100° C or less.

E. Thermomechanical modeling

According to thermal modeling, electrodes of the grid system are heated nonuniformly along the radius. This can cause thermomechanical deformation, which may lead to defocusing of the beam, as well as to the interelectrode gap reduction and interelectrode breakdown. Initial data defined by thermal modeling allow to solve the problem of thermal buckling of the grid system electrodes in geometrically nonlinear statement[16]. This allows to define the critical values of the radial temperature difference for the perfect flat electrodes, and to consider their behavior after the loss of stability. In addition, it is possible to make numerical study of nonlinear bending of electrodes more reasonably and effectively on the basis of the mathematical apparatus of boundary integral and integro-differential equations[17]. The following results were obtained by thermomechanical modeling: deflection of the accelerating electrode made of either molybdenum or titanium did not exceed 0.02 mm; deflection of the emission electrode made of molybdenum and titanium was 0.13 mm 0.98 mm, respectively. The titanium emission electrode can not be used as a part of the grid system for the RIT being developed because of too large deflection. In the case of molybdenum electrode, the deflection is acceptable. Deflection of the accelerating electrode has practically no effect on the ion beam focusing. Based on the results of thermomechanical modeling, we decided to make screen electrode of molybdenum and accelerating electrode of titanium. The choice of material for accelerating electrode is explained by the lower coefficient of ion sputtering of titanium compared to molybdenum[18].

III. Experimental development of the thruster

Table 2 presents main results of the low-power RIT experimental development. As is obvious from the Table, thruster performance are slightly lower the calculated values. This is due to the non-optimal design of the laboratory model. Rather high cost of propellant ionization is explained by the fact that the screen grid with 0.5 mm thickness was used in the laboratory model of the thruster. Reduction of ionization cost is expected with the screen grid thickness reduction down to 0.3 mm.

RF power, W	61.4
Ion beam current, mA	110
Accelerating voltage, V	2000
Propellant mass flow rate, mg/s	0.22
Mass efficiency	0.685
Specific thrust impulse, s	3775
Thrust, mN	8.1
Thruster power, W	281.4
Thruster efficiency	0.533
Propellant ionization cost	558

Table 2. Results of experimental development of low-power RIT

Conclusion

The radio-frequency low-power ion thruster was developed by the Moscow Aviation Institute in cooperation with OSC “KBKhA” for controlling of the orbital motion of small spacecraft. Basic thruster characteristics were calculated and basic mode of operation was selected. The basic geometrical parameters of the RIT grid system were calculated and the electrode configuration of the grid system was selected that allows to achieve rather narrow half-angle of divergence of the ion beam. Temperatures of the main structural elements of the thruster at the basic mode of operation were defined by thermal modeling. Thermomechanical calculation of the grid system was made based on the thermal simulation; according to it, molybdenum should be used as the material for the screen electrode, because when titanium was used for it, the electrode deflected substantially with heating, and that affected negatively the ion beam parameters.

The laboratory model of low-power RIT was made and its experimental development was conducted. Primary operating characteristics close to the calculated ones were received during tests. Optimization of thruster design and improvement of its characteristics continue.

Acknowledgments

This work was supported by the grant No. NSh-895.2014.8 of the Russian Federation President for the state support of the leading scientific schools of the Russian Federation; by the grant of the Russian Federation Government No. 11.G34.31.0022 for the state support of researches conducted under the supervision of the leading scientists at the Russian educational institutions of the higher professional education; with the state support for complex projects on creating high technology industries implemented with the participation of higher education establishments, agreement No. 02.G25.31.0072.

References

[1]Urlichich, Ju., Kuzenkov, A.. "Sputnikovaja svjaz': sostojanie i perspektivy," (Satellite communication – state and prospects") *Aerokosmicheskij kur'er*. 2012. No. 2. pp. 52–53 – in Russian.
[2]Zvezdin, I. "Malye kosmicheskie apparaty: perspektivy rynka," ("Small satellites – market trends") *Vzlet*. 2005. No. 1. pp. 50–55 – in Russian.
[3]Da Cilva Curiel, R.A. "SSHP-satellite classification" small satellites home page," Surrey Space Centre Nov. 2000.
[4]Reizniece-Ozola, D. "Business and legal aspects for small satellite control and payload data download using available commercial space-based communication systems," ISU EMBA 12 Module E –Thesis. 28 August 2012.
[5]Sevast'janov, N.N., Branec, V.N., Panchenko, V.A. "Analiz sovremennyh vozmozhnostej sozdanija malyh kosmicheskih apparatov dlja distancionnogo zondirovaniya Zemli," ("Analysis for the current feasibilities for creating spacecraft for remote Earth sensing"). *Trudy MFTI*. 2009. Vol. 1, No. 3. pp. 14–22 – in Russian.
[6]Loeb, H. W. "Development of RIT-Microthrusters," IAC-04-S.4.04. 55th IAC, Bremen, 2004.
[7]Abgaran, V.K. Akhmetzhanov, R.V., Loeb, H.W., Obukhov, V.A., Cherkasova, M.V. "Chislennoe modelirovanie pervichnogo puchka ionov i potoka vtorichnyh ionov v ionno-opticheskoj sisteme ionnogo dvigatelja," ("Numerical modeling for the primary ion beam and secondary ion flow in the ion-extraction system of ion thruster") Journal "*Trudy MAI*" [online journal], 2013. No. 71. URL: http://www.mai.ru/science/trudy/published.php?ID=46702 [cited 05 May 2015] – in Russian.
[8]Loeb, H. W. "Principle of radio-frequency ion thrusters RIT". RIT-22 demonstrator test of Astrium ST at University of Giessen, 06-11 September, 2010.
[9]Abgaran, V.K. Akhmetzhanov, R.V., Loeb, H.W., Obukhov, V.A., Cherkasova, M.V. "Numerical Simulation of a High-Perveance Ion-Optical System with a Plasma Emitter" *Journal of Surface Investigation. X-ray, Synchrotron and Neutron Techniques*. 2013. Vol. 7, No. 6. pp. 1092–1099.
[10]Akhmetzhanov, R.V., Loeb, H.W., Cherkasova, M.V., Obukhov, V.A. "Numerical Simulation of a System of Formation of an Intense Ion Beam From Gas Discharge Plasma of an Ion Thruster," the 64th International Astranautical Congress, Beijing, China, September 23-27, 2013, IAC-13-C4.4.11.
[11]Obukhov, V.A., Sosnovskij, V. E. "Raschet perehodnogo sloja v emissionnom otverstii gazorazrjadnogo istochnika ionov," ("Calculation for transition layer in the emissive hole of gas-discharge ion source") 5th Conference on Plasma Accelerators and Ion Injectors. 1982, pp. 105–106.
[12]The official website of IGUN software developer. URL: http://egun-igun.com [cited 05 May 2015].
[13]Goebel, D. M., Katz, I. "Fundamentals of electric propulsion," *JPL Space science and technology series*. March 2008. 493 pp.
[14]Loeb, H.W. "Radio Frequency Ion Beam Source" Pat. US5036252, Int. Cl. H01J 27/16, filed 1989.
[15] Birger, I. A. *Nekotorye matematicheskie metody reshenija inzhenernyh zadach*, ("Some mathematical methods for solving engineering problems") Moscow, Oborongiz, 1956. 150 pp. – in Russian.
[16]Birger, I. A. "*Kruglye plastinki i obolochki vrashhenija*," ("Round plates and shells of revolution"). Moscow, Oborongiz, 1961. 368 pp. – in Russian.
[17]Bezuhov, N.N. Bazhanov, V.L.,. Gol'denblat, I.I. *Raschety na prochnost', ustojchivost' i kolebanija v uslovijah vysokih temperatur.*("Calculation of strength, stability and oscillations under the high-temperature conditions") Moscow, Mashinostroenie, 1965. 567 pp. – in Russian.
[18] Zigmund, P. *Raspylenie tverdyh tel ionnoj bombardirovkoj ("*Solid body sputtering by ion bombardment"). Vol. I Moscow, Mir, 1984. pp. 23–98 – in Russian.